Available online at www.sciencedirect.com

ScienceDirect

Procedia Structural Integrity 18 (2019) 422–431

Structural Integrity Procedia

www.elsevier.com/locate/procedia

25th International Conference on Fracture and Structural Integrity

A numerical model based on ALE formulation to predict fast crack growth in composite structures

Francesco Fabbrocino[a] Marco Francesco Funari[b], Fabrizio Greco[b], Paolo Lonetti[b*] and Raimondo Luciano[c]

[a]*Department of Civil Engineering, Pagaso University, Centro Direzionale Isola F2, Naples 80143, Italy*
[b]*Department of Civil Engineering, University of Calabria, Via P. Bucci Cubo39B, Rende, Cosenza, 87030, Italy*
[c]*Department of Engineering, Partenope University, Centro Direzionale Isola C4, Naples 80143, Italy*

Abstract

A novel numerical strategy to predict dynamic crack propagation phenomena in 2D continuum media is proposed. The numerical method is able to simulate the behavior of materials and structures affected by dynamic crack growth mechanisms. In particular, an efficient computational procedure based on the combination of Fracture Mechanics concepts and Arbitrary Lagrangian and Eulerian approach (ALE) has been developed. This represents a generalization of previous authors' works in a dynamic framework with the purpose to propose a unified approach to predict crack propagation using dynamic or static fracture mechanics and a moving mesh methodology. The crack speed is explicitly evaluated at each time step by using a proper crack tip speed criterion, which can be expressed as function of energy release rate or stress intensity factor. In order to validate the formulation, experimental and numerical results available from the literature are considered. In addition, a parametric study to verify the prediction of proposed modeling in terms of mesh dependence phenomena, computational efficiency and numerical complexity is developed.

Peer-review under responsibility of the Gruppo Italiano Frattura (IGF) ExCo.

Keywords: Dynamic Crack Propagation, Moving Mesh, ALE, Finite Element Method.

* Corresponding author. Tel.: +390984496917;
E-mail address: lonetti@unical.it

1. Introduction

Nowadays, composite structures are widely used in several engineering applications ranging from civil, aerospace, marine etc. (Ascione et al. (2015), Barbero, et al. (2002),Bruno et al (2016), Funari et al (2018a), Ombres et al. (2019),

2452-3216
Peer-review under responsibility of the Gruppo Italiano Frattura (IGF) ExCo.
10.1016/j.prostr.2019.08.184

Funari and Lonetti, 2017). Due the high efficiency, composite materials are sometimes utilized under intensive loading conditions. This practice along with their heterogeneous nature can produce catastrophic failure modes (Camacho et al. (1996),), which might be affected by strong dynamic effects. To this end, several sophisticated numerical models able to simulate dynamic crack evolution are proposed in literature. Shahani et al. (2009) proposed a finite element model based on the re-meshing technique, which is able to predict both crack propagation and crack arrest in brittle materials. Despite high computational costs, re-meshing based methods have shown rigorous results to predict crack path and related fracture variables. Ooi et al (2013) implemented a methodology based on the Scaled Boundary Finite Element Method (SBFEM) for simulating dynamic crack propagation by adopting polygon elements. This numerical scheme presents a good capability for computing the fracture variables by means of re-meshing events. However, this produces changes to the global mesh, leading to large computation costs.

Zhang et al. (2019) developed an efficient numerical model consistent to the Cracking Elements (CE), which uses disconnected cracking segments to represent the fracture path. The main advantage of this approach is the absence of re-meshing or enrichments events, whereas the main disadvantages are the inability to accurately describe the crack tip position as well as stress intensity factors and energy release rate values.

Chen et al. (2019), De Maio et al. (2019), Feldfogel et al. (2019a), Feldfogel et al. (2019b), and Remmers et al. (2008) analyzed numerical models based on the Cohesive Zone Modelling (CZM), which were adopted for simulating crack evolution in both static and dynamic frameworks. An important advantage of the cohesive zone models is their ability to predict directly the crack onset and propagation, without introducing preexisting debonding length. However, the initial finite stiffness may produce, in brittle solids, an excess of compliance and in those cases in which a high stiffness is introduced spurious traction oscillations (Greco et al., 2015).

Recently, the use of Phase-Field Methods (PFM) has rapidly spread in view of its the capability to seamlessly deal with complex crack patterns like branching, merging and even fragmentation (Zhou et al. (2018), Staroselsky et al. (2019)). One of the main disadvantage of the phase-field approach is the fact that the method is still computationally intensive.

As a consequence, in order to avoid some of the issue previously mentioned, numerical models based on moving mesh methodology were developed. Lonetti (2010) proposed a model based on a combined approach developed in the framework of Fracture Mechanics and moving mesh methodology, which was able to predict dynamic delamination phenomena in layered structures. The same authors developed a numerical scheme based on a coupled approach between the moving mesh and the cohesive zone modelling (Funari et al. (2016)). In this case, moving mesh methodology based on ALE approach was introduced only for the interface regions, leaving the governing equations of the structural model, basically, unaltered.

It is worth noting that all these methods have their own advantages and disadvantages in terms of accuracy, stability, computational costs etc. The aim of the present work is to generalize the numerical approach developed in (Funari et al. (2019a)) to describe dynamic crack propagation in 2D media. This is achieved by introducing both crack propagation and direction criterions, appropriately. The work is organized as follows. Section 2 describes the model formulation. Section 3 illustrates the numerical results from a large parametric investigation. Finally, some remarkable conclusions are discussed in Section 4.

2. Formulation of the model

The proposed model represents a generalization of a previous authors work developed in a quasi-static framework (Funari et al. (2019b)). The governing equations of the structural model are defined by a classical formulation related to a 2D problem, essential and natural boundary conditions (Fig. 1):

$$div\left[\underset{\sim}{E}\ \underset{\sim}{\nabla}\underset{\sim}{u}\right]+\underset{\sim}{f}=\rho\underset{\sim}{\ddot{u}}\ \text{ in } V, \qquad \underset{\sim}{u}=\underset{\sim}{u}_c\ \text{ in } S_c, \qquad \left[\underset{\sim}{E}\ \underset{\sim}{\nabla}\underset{\sim}{u}\right]\underset{\sim}{n}=\underset{\sim}{p}\ \text{ in } S_p \tag{1}$$

Eq. (1) is integrated by boundary conditions, which define the crack path on the basis of a proper crack growth and direction criteria. Since the growth of an initial material discontinuity is simulated by the use of the ALE approach, the governing equations should be considered in terms of moving coordinates. According to ALE formulation, two

coordinate systems are introduced, known as Referential (C_R) and Moving (C_M) ones. The one to one relationship between the C_R and the C_M is defined by the mapping operator $\underset{\sim}{\Phi}$ (Funari et al. (2017), Lonetti et al. (2018)):

$$\underset{\sim}{X}_M = \underset{\sim}{\Phi}\left(\underset{\sim}{X}_R, t\right) \qquad \underset{\sim}{X}_R = \underset{\sim}{\Phi}^{-1}\left(\underset{\sim}{X}_M, t\right) \tag{2}$$

where $\underset{\sim}{X}_R$ and $\underset{\sim}{X}_M$ identify the positions on the computational points in C_R and C_M configurations, respectively. More details about the derivation of the governing equations of the problem are reported in (Funari et al. (2019)).

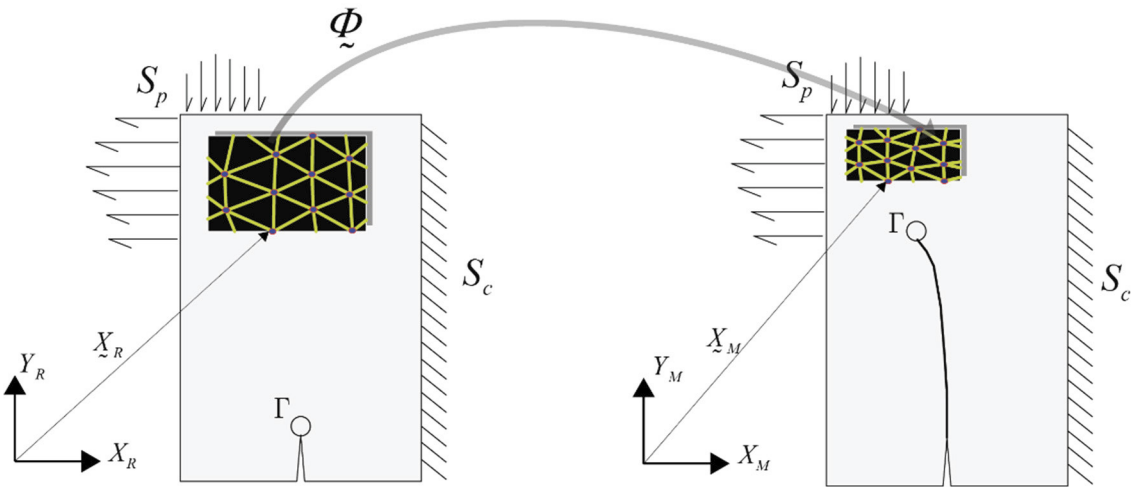

Fig. 1. Relationship between C_R and C_M coordinate systems.

According to ALE approach, the region enclosed into the Γ contour is able to describe the crack motion by introducing the following boundary conditions:

$$\Delta\dot{X}_T = \cos\theta_0\dot{\delta}_F, \quad \Delta\dot{Y}_T = \sin\theta_0\dot{\delta}_F, \tag{3}$$

where θ_0 is the crack propagation angle, whereas $\dot{\delta}_F$ is the incremental scalar quantity computed at the current iteration step, by adopting a proper dynamic crack growth criterion. The elements of the remaining regions of the structures are stretched due to the rezoning or regularization requirements, i.e. Laplace or Winslow methods, leading to a consistent transition mesh discretization (Funari et al (2018b)). It is worth noting how by adopting the following formulation, additional constraint conditions are needed to describe the crack growth by means of a tolerance angle criterion (Funari et. al (2019a)). It is worth noting that, when the tolerance criterion is satisfied a semi-automated re-meshing procedure is performed to transfer the nodal variables from the distorted (Moving system) to the new computational points (Fig. 2).

Governing equations as well as the computational steps described above, are implemented by adopting a proper script file written in MATLAB ® language which is linked to COMSOL Multiphysics FE software.

2.1. Crack motion and direction criterions

As reported in Nishioka (1997), for a non-self-similar fracture as curving crack growth, three types of numerical simulations can be adopted. The first type is the *generation phase simulation*, where the crack propagation is simulated by using both crack propagation and curved fracture path histories. The most used type of simulation adopted for curving crack growth is the *application phase simulation*, in which the numerical model needs two different criteria to determine the crack motion law as a function of the computed fracture variables and for predicting the direction of

the crack propagation (Bruno et al., 2005). Finally, in order to verify only the propagation-direction criterion shown in Nishioka (1997) a *mixed phase simulation* is adopted. In this case, the crack speed or the crack propagation increment is a-priori prescribed, whereas a propagation-direction criterion is implemented to compute the crack path on the basis of the fracture variables detected by the model. It is worth noting that the proposed model is quite general and the user might implement any kind of numerical simulation.

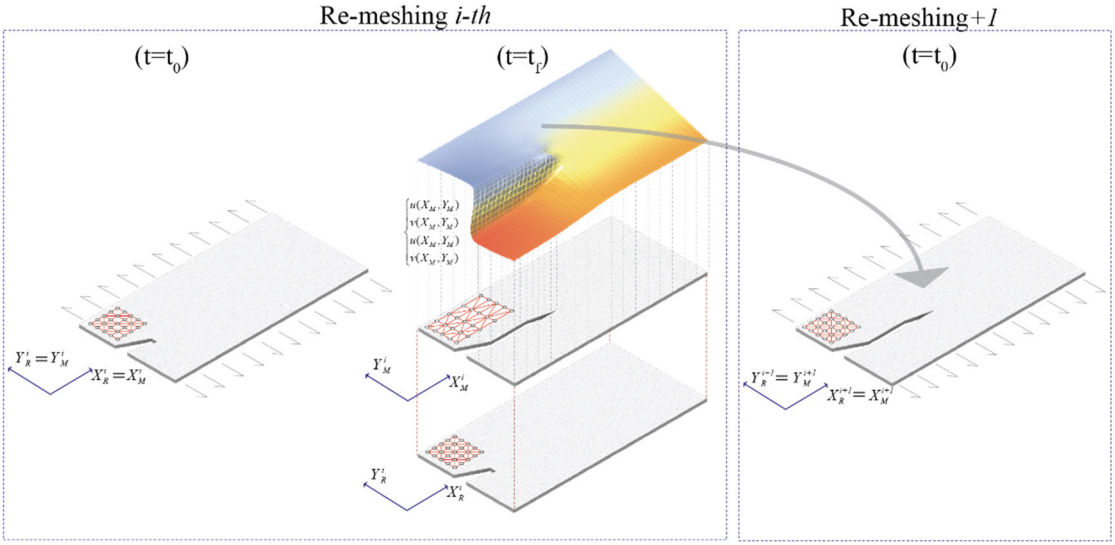

Fig. 2. Synoptic representation of the semi-automatic re-meshing: project process of the nodal variables from the distorted to the new computational points

In order to compute the ERR components G_1 and G_1, the equivalence to the path independent J integral developed by Nishioka (1997) has been integrated into the proposed numerical scheme:

$$\begin{aligned} J_k &= \lim_{\varepsilon\to 0}\int_{\Gamma_\varepsilon}\left[(W+K)n_k - t_i u_{i,k}\right]\mathrm{dS} \\ &= \lim_{\varepsilon\to 0}\left\{\int_{\Gamma+\Gamma_c}\left[(W+K)n_k - t_i u_{i,k}\right]\mathrm{dS} + \int_{V_\Gamma - V_\varepsilon}\left[(\rho\ddot{u} - f_i)u_{i,k} - \rho\dot{u}_i\dot{u}_{i,k}\right]\mathrm{dV}\right\} \end{aligned} \tag{4}$$

where Γ_ε is a contour close to the crack tip, W and K are the strain and the kinetic energy densities and n_k are outward normal direction cosines; u_i, $\dot{u}_i$ and $\ddot{u}_i$ are the displacement velocity and acceleration of the material point; ρ is the material density, Γ is an arbitrary contour, which goes around the crack tip. In order to compute numerically the ERR, path independent J integral is developed consistently to the expression provided in Nishioka (1997), here reported for completeness:

$$J_k = \int_{\Gamma+\Gamma_c}\left[(W+K)n_k - t_i u_{i,k}\right]\mathrm{dS} + \int_{V_\Gamma}\left[(\rho\ddot{u} - f_i)u_{i,k} - \rho\dot{u}_i\dot{u}_{i,k}\right]\mathrm{dV} \tag{5}$$

The ERRs components, evaluated with reference to the global coordinates system, can be projected on the local tip coordinates by using the following coordinate transformation rules:

$$\begin{bmatrix} J_x \\ J_y \end{bmatrix} = \begin{bmatrix} \cos\theta_0 & \sin\theta_0 \\ -\sin\theta_0 & \cos\theta_0 \end{bmatrix}\begin{bmatrix} J_X \\ J_Y \end{bmatrix} \tag{6}$$

thus:

$$J_x = \cos\theta_0 J_X + \sin\theta_0 J_Y$$
$$J_y = -\sin\theta_0 J_X + \cos\theta_0 J_Y \tag{7}$$

where J_x is the tangential component of the dynamic J integral. J_x corresponds to the rate of change in the potential energy per unit crack extension and it represents the dynamic ERR (Nishioka (1997)).

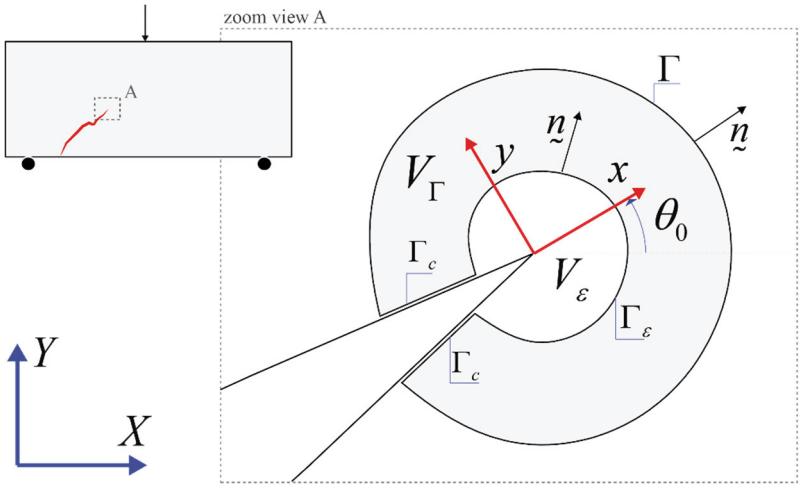

Fig. 3. Schematic representation of the path independent J integral developed by Nishioka (1997).

The computation of the SIFs has been done by using the component separation method proposed by Nishioka et al. (1997), where K_I and K_{II} expressions are related to the dynamic J integral, crack velocity parameters and crack velocity functions.

In order to compute the crack propagation direction a proper crack kinking criterion has to be considered. the proposed model incorporates Maximum Energy release rate criterion which is simply defined as:

$$\theta_0 = \tan^{-1}\left(\frac{J_Y}{J_X}\right) \tag{8}$$

in which θ_0 is measured with respect the horizontal global axis (Fig. 3).

3. Results

The following numerical simulations investigate the Araldite-B rectangular double cantilever beam, which was experimentally tested by Kalthoff et al. (1977). The loading, boundary conditions and geometry configuration are represented in Fig. 4, whereas the mechanical parameters are summarized in Table. 1.

Numerical and experimental data are collected by means of a two-step analysis. The first one is needed to load the structure by means a static analysis in which a vertical displacement at the pin is applied until the mode I SIF reached a value corresponding to the initial SIF detected by Kalthoff et al. (1977). At this stage, the total elastic energy of the structure is accumulated. Once the SIF reaches the prescribed value, a restart procedure is achieved and the crack propagation is enforced by the activation of the crack growth criterion. In particular, the $c - K_I^{dyn}$ curve experimentally determined by Kalthoff et al. (1977) is implemented to compute the crack tip velocity at each time increment of the simulation (Fig. 5). According to Nishioka (1997) classification, an *application phase simulation* is developed. It is

worth nothing that, in the present loading scheme, the crack propagates forward along the horizontal direction, leading the crack angle always equal to zero.

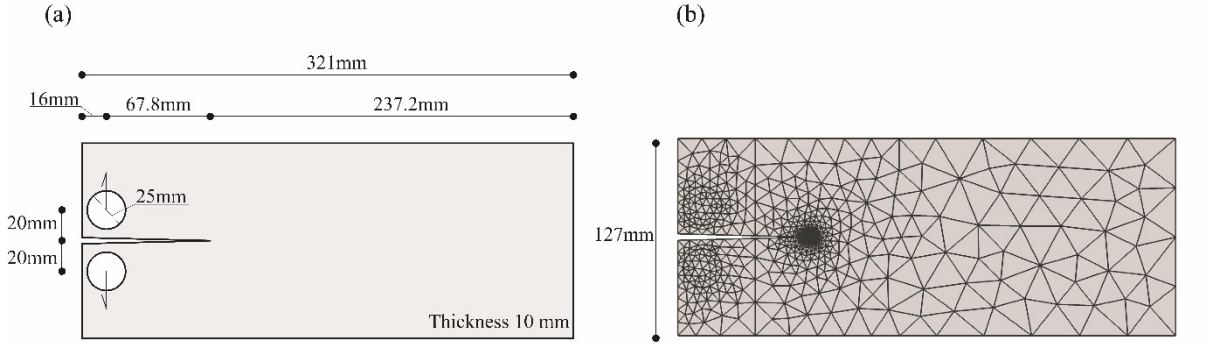

Fig. 4. Araldite-B rectangular double cantilever beam: (a) geometry and loading configuration; (b) intial mesh configuration.

Table 1. Mechanical properties of Araldite-B.

E (MPa)	ν	μ (MPa)	ρ (kg m^{-3})
3660	0.39	1316	1172

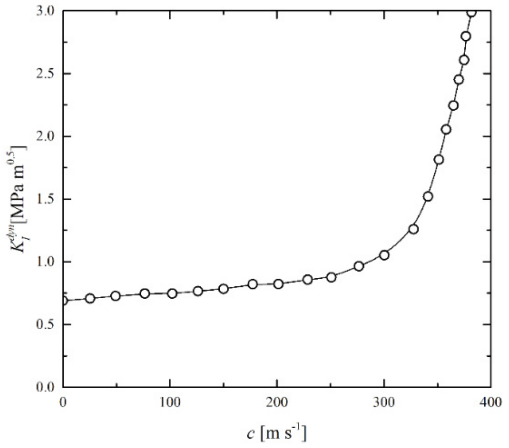

Fig. 5. Dynamic fracture toughness vs. crack tip speed for Araldite-B.

The dynamic behavior of the structure is analyzed by means three different loaded configurations, which are featured by the initial values of SIF reached during the static loading step:

- $K_I = 2.32$ MPa m$^{0.5}$ (L1)
- $K_I = 1.76$ MPa m$^{0.5}$ (L2)
- $K_I = 1.33$ MPa m$^{0.5}$ (L3)

Fig. 4b represents the mesh discretization adopted for the numerical simulations, in which a relatively refined mesh is considered just around the crack tip region, whereas the remaining part of the structures presents a transition mesh.

In Figs. 6a, 6b and 7a, results in terms of crack velocity as a function of the crack tip position obtained by the proposed model are compared with existing experimental (Kalthoff et al. (1977)) and numerical (Shahani et al. (2009) and Ooi et al (2013)) data. The curves show high values of the crack tip speed expecially during the initiation phase. Once the crack tip moves an oscillatory behavior is observed until the crack arrest phenomenon is achieved.

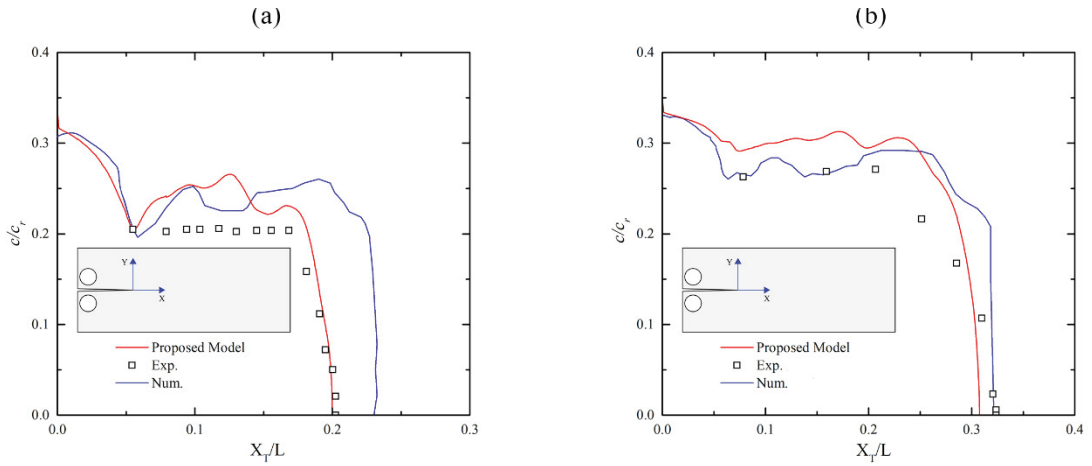

Fig. 6. Crack tip speed vs crack tip position, comparisons with numerical (Shahani et al. (2009)) and experimental (Kalthoff et al. (1977)) data: (a) L1 loaded configuration; (b) L2 loaded configuration.

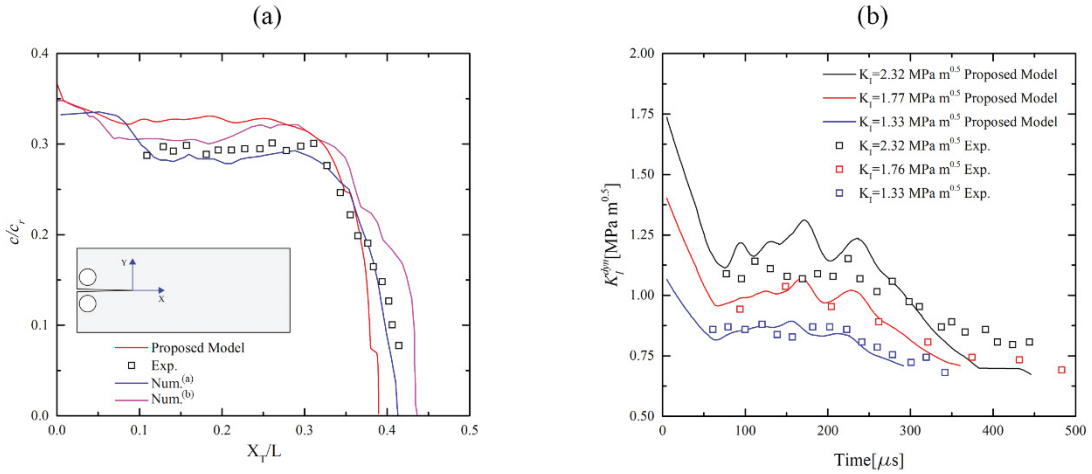

Fig. 7. (a) Crack tip speed vs crack tip position: comparisons with numerical (Shahani et al. (2009), Ooi et al (2013)) and experimental (Kalthoff et al. (1977)) data; (b) Variation of dynamic stress intensity factor vs time: comparisons with experimental data (Kalthoff et al. (1977)).

In Fig. 7b, the dynamic SIF time history computed by means of the proposed model, for the three loading configurations, are compared with experimental data (Kalthoff et al. (1977)). The numerical results are in good agreement with the data arising from the experimental (Kalthoff et al. (1977)) and numerical (Shahani et al. (2009) and Ooi et al (2013)) results taken from literature.

All the computations are performed on a Xeon processor running on a Windows 10 system. The governing equations are solved by using an implicit time integration scheme based on a variable step-size backward differentiation formula (BDF). The total computational time used by the proposed numerical scheme is about 700 s, while it is about 360000 s for the re-meshing technique developed by Shahani et al. (2009). Thus, this formulation allows to save much of the total computational time.

In order to verify the computational efficiency of the proposed model, the influence of the mesh discretization as a function of both the mesh dependency and computational costs are discussed. To this end the following mesh discretization are considered:

- characteristic length equal to $\Delta D / R = 1/3$ in the tip region and transition mesh in the remaining part of the plate with maximum length equal to $\Delta D / R = 20/1$ (M1).
- characteristic length equal to $\Delta D / R = 1/4$ in the tip region and transition mesh in the remaining part of the plate with maximum length equal to $\Delta D / R = 15/1$ (M2).
- characteristic length equal to $\Delta D / R = 1/4$ in the tip region and transition mesh in the remaining part of the plate with maximum length equal to $\Delta D / R = 3/1$ (M3).

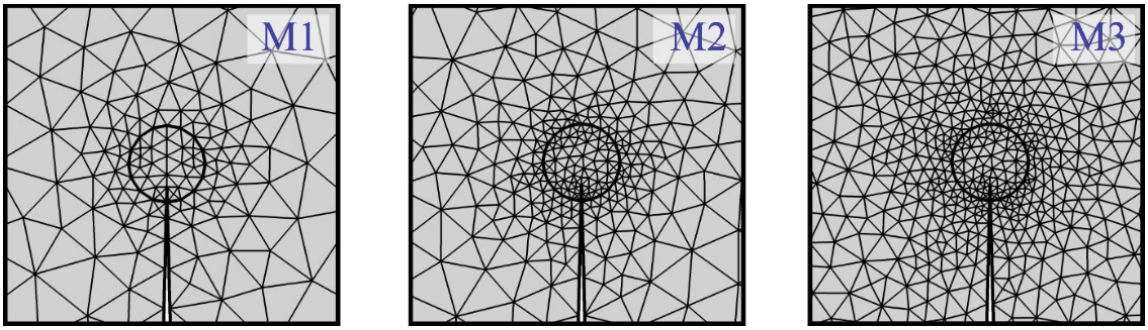

Fig. 8. Mesh discretizations detail around the crack tip for M1, M2 and M3 configurations.

Fig. 8 shows the mesh discretization around the crack tip region for M1 M2 and M3 configurations. In this case the numerical simulations are employed by considering the loading condition with $K_I = 1.33$ MPa m$^{0.5}$. Fig. 9 investigates the computational efficiency in terms of both CPU time and DOFs. The results show how adopting a relatively coarse discretization, i.e. M1 and M2, it allows to save a significant amount of the computational time by 77% and 44% with respect to the M3 configuration.

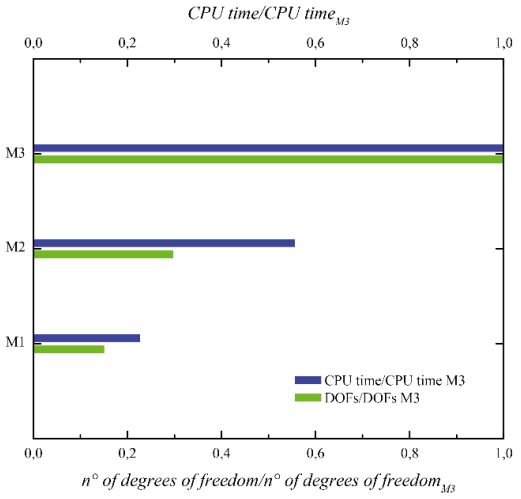

Fig. 9. Comparisons in term CPU time and number of degrees of freedom for the numerical simulation performed by using different mesh discretizations (M1, M2 and M3).

In Fig. 10a, comparisons in terms of crack tip speed as a function of the crack tip position, for each mesh configurations, are reported. The results show how the proposed model is able to describe efficiently dynamic crack propagation phenomena by using a relatively coarse discretization.

The results, reported in Fig. 10b, show relative low discrepancies in the prediction of the dynamic SIFs history and therefore it confirms a mesh independent behavior, since a coarse discretization (M1) is able to detect accurately the fracture variables. Fig. 11 shows a synoptic representation of the mesh motion during the crack propagation for the M1 configuration. This result shows how the mesh movements of the crack tip region are enforced rigidly ensuring accuracy in the prediction of the fracture variables and a reduced level of mesh dependency.

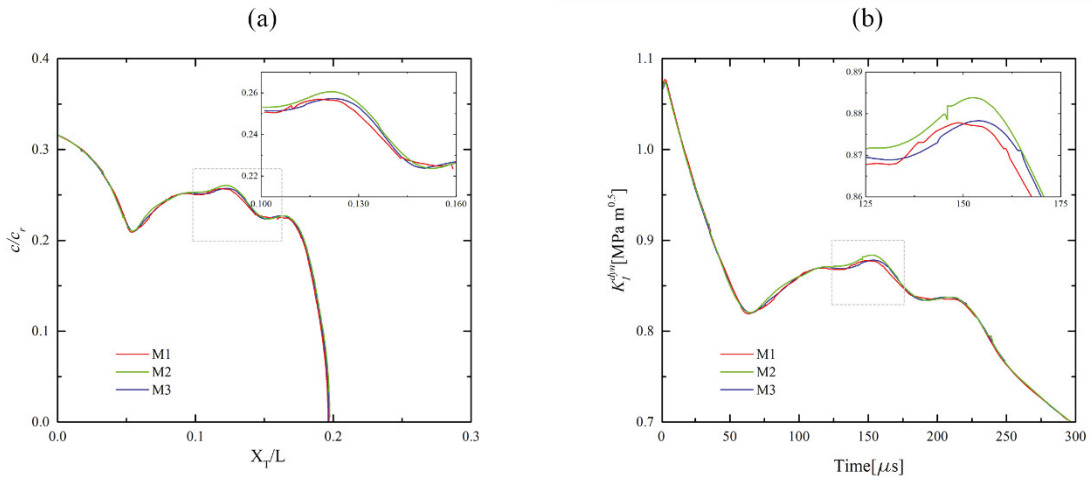

Fig. 10. (a) Crack tip speed vs crack tip position and (b) variation of dynamic stress intensity factor vs time for the numerical simulation performed by using different mesh discretizations (M1, M2 and M3).

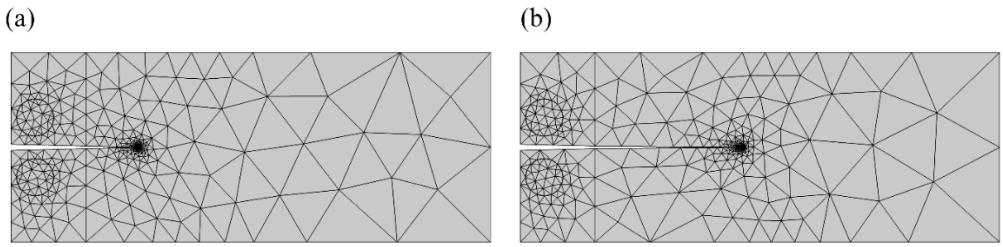

Fig. 11. Synoptic representation of the mesh motion during the crack propagation for the M1 mesh configuration.

4. Conclusions

Dynamic crack propagation phenomena are successfully simulated by using a new numerical methodology which combines concepts arising from solid mechanics, fracture mechanics and moving mesh methodology. The numerical formulation is able to describe crack propagation just by adopting a proper crack function and kinking criterion. Although the numerical scheme allows to describe crack curving phenomena, the numerical validation is developed with reference to several loading schemes. The validity of the proposed model was proved by means of comparisons with experimental and numerical data taken from the literature, denoting computational efficiency, accuracy and robustness of the numerical formulation.

References

Ascione, L., Berardi, V.P., Giordano, A. & Spadea, S., 2015. Pre-buckling imperfection sensitivity of pultruded FRP profiles", Composites Part B: Engineering 72, 206-212.

Barbero, E.J., Lonetti, P., 2002. An inelastic damage model for fiber reinforced laminates. Journal of Composite Materials. 36, 941-962.

Bruno, D., Lonetti, P., Pascuzzo, A. 2016, An optimization model for the design of network arch bridges, Computers and Structures, 170, 13-25.

Bruno, D., Greco, F., Lonetti, P., 2005. Computation of energy release rate and mode separation in delaminated composite plates by using plate and interface variables. Mechanics of Advanced Materials and Structures, 12 (4), 285-304.

Camacho, G.T., Ortiz, M., 1996. Computational modelling of impact damage in brittle materials. International Journal of Solids and Structures 33, 2899-2938.

Chen, S., Mitsume, N., Gao, W., Yamada, T., Zang, M., Yoshimura, S., 2019. A nodal-based extrinsic cohesive/contact model for interfacial debonding analyses in composite structures. Computers and Structures 215, 80-97.

COMSOL, COMSOL Multiphysics® v. 5.2, www.comsol.com. 2015: COMSOL AB, Stockholm, Sweden.

De Maio, U., Fabbrocino, F., Greco, F., Leonetti, L., Lonetti, P., 2019. A study of concrete cover separation failure in FRP-plated RC beams via an inter-element fracture approach. Composite Structures 212, 625-636.

Feldfogel S., Rabinovitch, O., 2019. Crack induced interfacial debonding in damaged RC slabs strengthened with FRP. International Journal of Fracture 215, 153-173.

Feldfogel S., Rabinovitch, O., 2019. Two Dimensional Dynamic Debonding in FRP Strengthened Plates. International Journal of Solids and Structures, Accepted Manuscript

Funari, M.F., Lonetti, P., 2017. Initiation and evolution of debonding phenomena in layered structures, Theoretical and Applied Fracture Mechanics 92, 133-145.

Funari, M.F., Greco, F., Lonetti, P., 2016. A moving interface finite element formulation for layered structures. Composites Part B: Engineering 96, 325-337.

Funari, M.F., Greco, F., Lonetti, P., 2017. Dynamic debonding in layered structures: A coupled ALE-cohesive approach. Frattura ed Integrita Strutturale 41, 524-535.

Funari, M.F., Greco, F., Lonetti, P., Luciano R., Penna R., 2018. An interface approach based on moving mesh and cohesive modeling in Z-pinned composite laminates. Composites Part B: Engineering 135, 207-217.

Funari, M.F., Greco, F., Lonetti, P., 2018. Sandwich panels under interfacial debonding mechanisms. Composite Structures 203, 310-320.

Funari, M.F., Greco, F., Lonetti, P., Spadea, S., 2019. A numerical model based on ALE formulation to predict crack propagation in sandwich structures. Frattura ed Integrita Strutturale 13 (47), 277-293.

Funari, M.F., Lonetti, P., Spadea, S., 2019. A crack growth strategy based on moving mesh method and fracture mechanics. Theoretical and Applied Fracture Mechanics 102, 103-115.

Greco, F., Leonetti, L., Lonetti, P., 2015. A novel approach based on ALE and delamination fracture mechanics for multilayered composite beams. Composites Part B: Engineering, 78, 447-458.

Lonetti, P., 2010. Dynamic propagation phenomena of multiple delaminations in composite structures. Computational Materials Science 48 ,563-575.

Lonetti, P., Maletta, R., 2018. Dynamic impact analysis of masonry buildings subjected to flood actions. Engineering Structures 167, 445-458.

Nishioka, T., 1997. Computational dynamic fracture mechanics. International Journal of Fracture 86, 127-159

Ombres, L., Mancuso, N., Mazzuca, S., Verre, S. 2019. Bond between carbon fabric-reinforced cementitious matrix and masonry substrate. Journal of Materials in Civil Engineering 31.

Ooi, E.T., Shi, M., Song, C., Tin-Loi, F., Yang, Z.J., 2013. Dynamic crack propagation simulation with scaled boundary polygon elements and automatic remeshing technique. Engineering Fracture Mechanics 106, 1-21.

Remmers, J. J. C., de Borst, R., Needleman, A., 2008. The simulation of dynamic crack propagation using the cohesive segments method. Journal of the Mechanics and Physics of Solids 56, 70-92.

Shahani, A.R., Amini Fasakhodi, M.R., 2009. Finite element analysis of dynamic crack propagation using remeshing technique. Materials and Design 30, 1032-1041.

Staroseldky, A., Acharya, R., Cassenti, B., 2019. Phase field modeling of fracture and crack growth. Engineering Fracture Mechanics 205, 268-285.

Zhou, S., Zhuang, X., 2018. Adaptive phase field simulation of quasi-static crack propagation in rocks. Underground Space 3, 190-205.

Zhang, Y., Zhuang, X., 2019. Cracking elements method for dynamic brittle fracture. Theoretical and Applied Fracture Mechanics 102, 1-9.